Early-season Vineyard Shoot and Leaf Estimation Using Computer Vision Techniques

HARJATIN SINGH BAWEJA[1 *], TANVIR PARHAR[2 *], STEPHEN NUSKE[3]

[1,2,3]Robotics Institute, Research Associate, Carnegie Mellon University, 5000 Forbes Avenue, Pittsburgh, 15232,
United States of America
E-MAIL: harjatis@andrew.cmu.edu, ptanvir@andrew.cmu.edu, nuske@cmu.edu

Abstract:

This paper describes computer vision techniques for early-season measurement of vine canopy parameters; leaf count, leaf area and shoot count. Accurate and high-resolution estimation of these key vineyard performance components are important for effective precision management. We use a high-resolution stereo camera with strobe lighting mounted on a ground-vehicle that captures high-quality proximal images of the vines. For shoot image segmentation, we apply the Frangi vessel filter (originally developed for medical imaging processing) in conjunction with custom filtering to extract shoot counts. We also present an incremental leaf count estimation algorithm, that proposes leaf candidates for incremental leaf sizes and then removes the repeating candidates to accurately assess leaf count. The specified algorithms are robust to partial occlusion and varying lighting conditions. For shoot count measurement we observe an F1 score of 0.85 for image shoot count and R correlation of 0.88 for ground-truth shoot counts. The R correlation for leaf count estimation between ground truth sample images and algorithm output is 0.798. Whereas the R correlation between the data collected by a PAR sensor and leaf area estimation algorithm is 0.69.

Keywords:

Plant Segmentation; Computer Vision; Image processing; Precision Viticulture; Precision management; Shoot Count; Leaf Count; Leaf Area;

1. Introduction

Vineyard cultivation industry is a large and diverse industry. As many as 40 different varieties of grapes are known and cultivated worldwide. The produce is used for production of various edibles like grape juice, raisins and wine. As reported by “International Organization of Wine and Vine”, as of 2015 vineyards covered 7.534 million hectares of agricultural land worldwide. To give a better perspective to the size of the industry, according to “The Wine Institute from TTB data”, the total wine produced by USA alone was 835.468 million gallons. Hence, such high investments and stakes involved in the vineyard industry makes application of technological advances in vineyard management a valuable exercise.

Currently there are no systems available for growers to measure crop yield with high resolution during the growing season. Crop yield is a desirable attribute to be monitored and managed. The current process to estimate yield is by monitoring the farm at harvest time, and recording data during each growing season. However, yield can vary by large amounts from year to year, and using harvest estimates is an extremely coarse approximation of yield. In order to get accurate dense measures of crop yield, the crop needs to be continuously measured during the growing season. The obvious solution would be to exhaustively monitor the fields.

While the approach might work well for small sized fields, it becomes economically intractable for larger fields owing to the labor intensive nature of the work. Additionally, the manual counting mechanism is performed just before harvest. Over the past few years, our research group has focused on developing a vision-based system for automatic fruit detection and high resolution yield-estimation [1] [2]. However, this does not include two of the major components of yield estimation and crop management, namely shoot density and leaf area and count measurements.

One of the most major components of precise yield management is shoot density estimation for vines across the field. An accurate machine vision based approach for efficient calculation of this parameter would not only giving a vital estimate of number of prospective fruit bearing healthy crops this season but also be a telling parameter to monitor plant growth and health. Leaf area and leaf count estimation, during the early growth season helps the farmer to get a better insight

* : THE AUTHORS HAVE CONTRIBUTED EQUALLY.

into vineyard's overall health. Providing a farmer with geo-localized maps of leaf count/area help the farmer in focusing the water and nutrient resources. This in turn helps in an increase in the yield. The reduction and optimization of resources used in vineyard management is the motivation behind this work

2. Related Work

Exponentially increasing population growth has resulted in the need for proportionate increase in agricultural produce as well. Though population is growing at an exponential rate, the same cannot be said for cultivatable land. Thus this creates a need for increasing output from currently available land without overburdening it. This has led to an increased interest in funding research in precision viticulture.

Some work has been done to obtain precise yield estimates in vineyards by accurately measuring fruit density measurement using classical image processing techniques [9][10]. There have also been some successful attempts at using purely learning based techniques such as feature-learning based techniques [4], conditional random fields(CRFs) [5] amongst others. However, the most successful have been the ones using a combination of classical image processing pipelines with learning based methods [2].

Surprisingly very little work is done on using shoot density measurement and leaf area/count estimates to do the same work. Some thinning based techniques have been used to remove shoots from the rest of the plant and estimate density [3]. There also has been an attempt at using reflection patterns of structured light to delineate convex shapes from concave ones thus using this technique to segment shoots from rest of the plant. [5]. Shape fitting based stem segmentation techniques on 3 dimensional plant models by taking advantage of prior knowledge of plant structure have also been attempted. [6]. The most promising approach is use of vesselness measure of plant branches for segmentation [21]. The method provides promising results in lab conditions, however uses the assumption that size of plant shoot is considerably larger than the size of leaf edges which is subject to plant type and not robust to occlusions. Thus, this paper uses the work of Amean et.al. [21] as baseline for shoot density measurement and builds on that.

There have been a wide variety of attempts for estimation of leaf count and leaf area of plants. Various methods deploy techniques varying from image processing methods to digital sensor based data acquisition techniques. There has been an attempt on leaf segmentation by fitting quadratic curves to a combination of depth data and IR data [11]. RGBD sensors like Microsoft Kinect have been used for leaf segmentation and leaf count estimation using center of divergence methods, which employ parametric snakes [12][13]. But the drawback of this approach is limitation of Kinect to indoors and the slow convergence of parametric snakes. There exist techniques involving a combination of log-polar transformation and unsupervised learning using triangle encoding and K means clustering [14, 15, 16]. But these techniques presume that leaves are of a distinct shape, like circular or elliptical. Active Shape Modelling [17] technique has been used to detect multiple leaves, which might be occluded. The leaf boundaries and veins are detected using gradient change. Since this method tries to fit a model to leaves, it assumes all leaves to be roughly of similar shape. This is highly unlikely in the case of grape vines in outdoor conditions.

Various techniques have been developed for leaf and canopy area estimation. NDVI [18] and PAR [19] sensors are known to be deployed over the field for vegetation index measurement. While they are straightforward to use, they are prone to errors due to change in distance from the vine under scrutiny. A machine learning based approach that estimates leaf area based from RGB images has also been tested [20]. One major drawback again, is the distance of camera from vines must remain unchanged.

Though abovementioned works have been successfully implemented and display high accuracy, all of them have been tested on datasets obtained in favorable controlled lab environments. Thus making them vulnerable to failure in nonstandard conditions with varying lighting conditions, occlusions and scales. The major problem with leaf count estimation of grape vine leaves in field environments is clutter and background noise. The indefinite shape of leaves due to occlusion and curling further thwarts the process.

3. Approach

Our custom camera setup, mounted on a farm vehicle captures high resolution RGB stereo images. These images are used for all image based inferences. The depth generated from these images is used to convert inferred data into metric units. The images produced are not aligned to each other at first, hence they are first rectified, for accurate depth map estimation.

3.1 Disparity calculation

After rectification, the correspondence problem can be solved by using an algorithm whose job is to scan both the images for matching features. Algorithms like Block Matching use a small patch around a pixel in one image and then look for the best match along the epipolar line for all possible values of disparities.

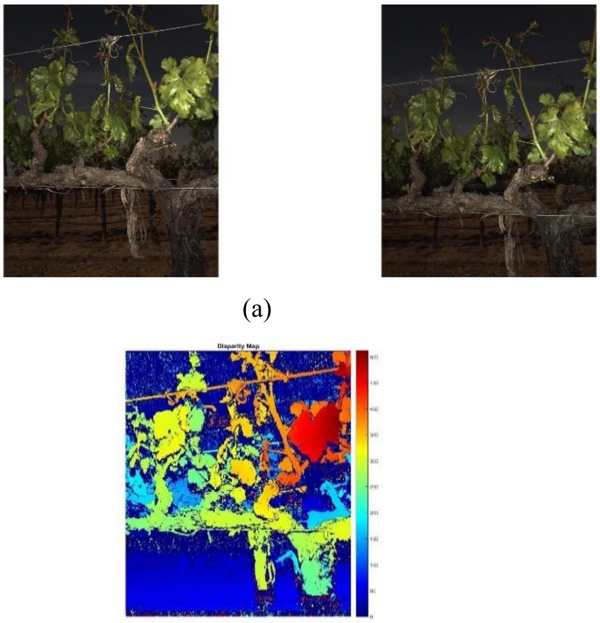

(a)

(b)

FIGURE 1 Top two images in (a) represent the stereo image pair while image (b) is the corresponding disparity map

A comparison between the two patches in the images is made by comparing the corresponding pixels in the two patches, according to Normalized Correlation

$$\text{N.R} = \frac{\sum\sum L(r,c) \quad . \quad R(r,c-d)}{\sqrt{(\sum\sum L(r,c)^2 \quad . \quad (\sum\sum R(r,c-d)^2)}} \qquad (1)$$

Where L: left image patch R: right image patch r: row number c: column number d: current disparity. The disparity for which N.R is least being the disparity of the current pixel.

Using disparity we can calculate real world X,Y and Z using the relations (2) (3) and (4). Here f is camera’s focal length, B is camera baseline and D is the disparity. U and V are pixel coordinates in X and Y directions respectively.

$$Z = \frac{fB}{d} \qquad (2)$$

$$X = \frac{uZ}{f} \qquad (3)$$

$$Y = \frac{vZ}{f} \qquad (4)$$

The disparity map and corresponding stereo image pair is displayed in Figure 1. All the points that have a depth above a certain threshold are removed. Thus, segmenting the background.

3.2 Color Segmentation

The first step is to pre-process the image by removing the background as well as the non-green parts of the image. Hence, first the image is converted from RGB color space to HSV color space, so that the thresholding is easier and provide robustness to varying lighting conditions

Then the HSV image is thresholded such that Hue value is between 0.1 and 1, saturation values are between 0.25 and 1. Figure 2 shows image after color segmentation and contrast stretching.

3.3 Frangi filter

As per the approach suggested by Amean et.al. [21], we use Frangi 2D filter to obtain vessel like structures (shoots in our case) by use of eigenvalues of the Hessian matrix of pixel intensities as suggested by Frangi et al. [7]:

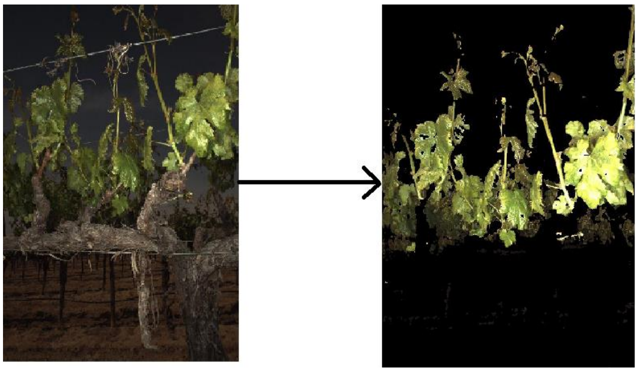

FIGURE 2. Left side is the initial image and right side is the image after background removal and color segmentation

$$H = \begin{bmatrix} I_{xx} & I_{xy} \\ I_{yx} & I_{yy} \end{bmatrix} \qquad (5)$$

I is the pixel's intensity value. The image's second order derivatives are calculated by convolving the image with derivatives of a Gaussian kernel. A small first eigen value of the corresponding Hessian and a large second eigen value are suggestive of a 'tube-like' structure (in our case, shoots). Figure 3 shows the output of the applied filter on previously enhanced image and thresholding the grayscale image to obtain a binary image.

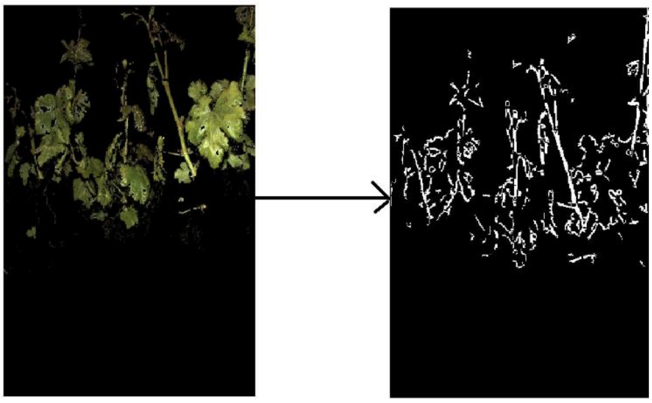

FIGURE 3. Left side is the segmented image and right side is the image after applying Frangi image.

3.4 Hough Transforms

Hough Transforms [Duda and Hart, 8] is a popular technique to detect imperfect shapes in an image. It involves using parametric form of figures and a voting mechanism to determine how many points in the image fall on the specified parametric curve. If the number of points falling on the curve are above a predefined threshold, the curve is said to exist in the figure. Hough line detection is used on the output binary image obtained in the previous step to obtain all the candidate shoots in the image. Figure 4 shows the output of Hough line detection applied to the output obtained in previous step.

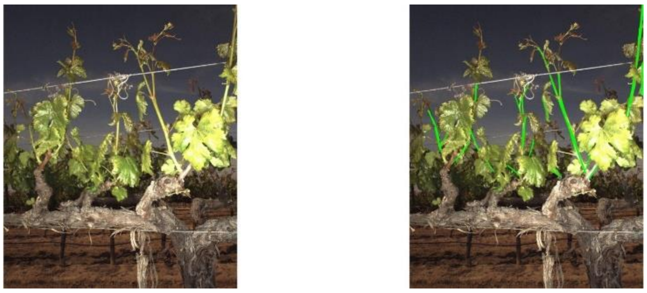

FIGURE 4. Left side is the segmented image and right side is the image after applying Hough transform on Frangi image

3.5 False positive removal

It can be observed that if length of Hough line is set as the only criteria to separate shoots from leaf edges, it is certain to miss the shoots occluded by leaves. If not, the output consists of several false positive in the form of leaf edges. In order to obtain high precision, the length threshold is kept to a bare minimum and custom filters are applied to remove false positives.

3.5.1. Perpendicular intensity profile

We have all the Hough lines; we divide these each Hough line into 5 equal segments. At each segment we make an intensity profile across the Hough line and analyze it. To make the analysis robust to minor variations, we first fit a polynomial on the intensity profile. It can be intuitively seen that in case of leaf edges this profile will be a monotonically increasing or decreasing and in case of shoot a bell shaped curve should be observed.

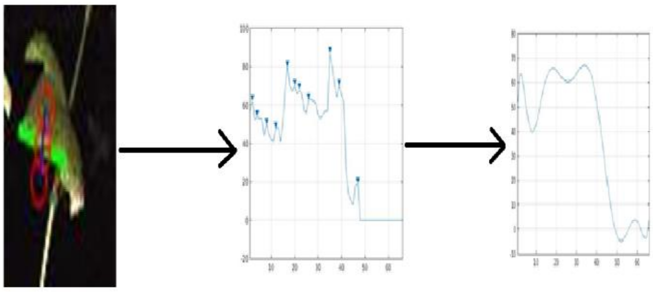

(a)

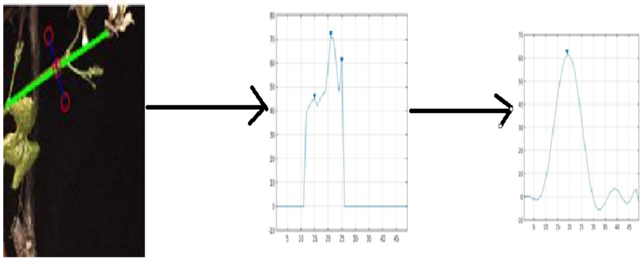

(b)

FIGURE 5 (a) Perpendicular intensity profile for leaf (b) Perpendicular intensity profile for shoot

If for a majority of intensity profiles, a monotonic increase or decrease is observed, then it is said that the given Hough line is a false positive. Figure 5 shows the perpendicular intensity profile results for both a leaf and a shoot.

3.5.2. Parallel intensity profile

We make an intensity profile along the length of the Hough line (green line) output from previous step. It is observed that the intensity profile for actual shoots if a lot smoother whereas intensity profile for leaf edges has a lot more jitter. Thus we obtain the intensity profile along the Hough line and fit a polynomial to it in order to smoothen the function. Then peak analysis is done on this intensity profile.

Thus we try and find all the peaks which have prominence more than one fourth of the average intensity in that intensity profile. If we find more than 2 such peaks, we reject the Hough line.

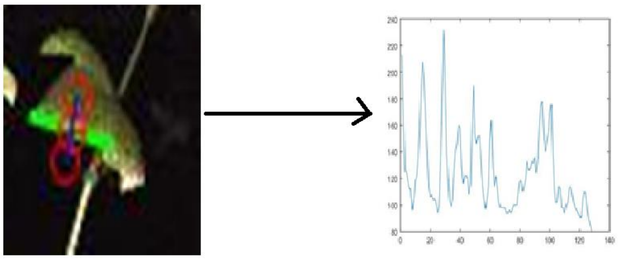

(a)

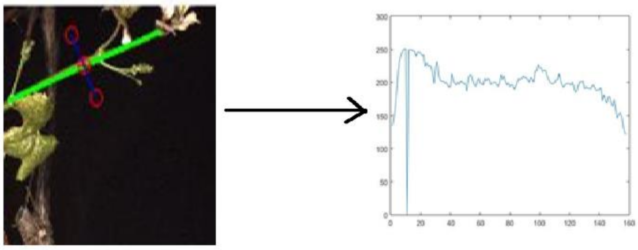

(b)

FIGURE 6 (a) Parallel intensity profile for leaf (b) Parallel intensity profile for shoot

3.6 Multiple detection removal in shoots

It can very often be the case that a shoot is detected multiple times, i.e. there are multiple lines describing the same shoot. One most obvious scenario is when a shoot is partially occluded by a leaf in the middle. To remove these multiple detections, we have the following approach. We start by doing blob analysis on binary mask of the selected Hough lines. We start by getting all connected components in the binary mask with the following algorithm.

Blobs are the continuous regions in the black and whire binary image mask. Using matlab BlobAnalyser, we detect blobs from sizes ranging from 1000 px^2 to 50000 px^2. This gives us all the continuous regions in the image, with almost all possible sizes.
For blob analysis the following algorithm is followed :

1. We start with the first foreground pixel in the binary image. We assign the label "current_label" to 1. Then go to 2

2. If the current pixel is a foreground pixel and is currently unlabeled, then give it the label name "current_label". Put it as the current element in the queue. If it is not a foreground pixel, then repeat this step for next pixel.

3. Then take out an element from the queue and analyze the neighbours, based on either 4-Connectivity or 8-Connectivity. If the neighbour is not a background and not currently labeled, then give it the label "current_label". And add it to the queue. Repeat it until there remain no more elements in the queue.

4. Then go to second step for the bext pixel in the image and increase the "current_label" by 1.

Hence, the above algorithm gives us the connected components in the binary mask. These components are further analyzed to remove all the prospective multiple detections.

Then this is followed by ellipse fitting on all the connected components. The following steps are followed to remove double detections.

1. Treat every connected component as a separate ROI(Region of interest)

2. Locate center of mass for each ROI and locate each pixel in ROI with respect to center of mass

3. Use Eigen values of the mass distribution tensor of these pixels to get ellipse orientation, minor and major axis [22].

4. If two ellipses are of similar orientations, then transform coordinate system to align with ellipse's orientation. In order to remove double detections, if horizontal distance between two ellipses' centers is very small in the transformed coordinate system, they are said to be parts of a common shoot.

The image pipeline in figure 7 well describes the entire process, of how first each segment is taken as individual region of interest. Then ellipse is fit on each of these segments. Then if any two ellipses have similar orientations, these ellipses are candidates for being the same shoot. After this the coordinate system is shifted to be aligned with ellipse's major axis. If two ellipses have similar orientation and the horizontal distance between their centroids is small in the transformed coordinate system then these two ellipses are merged, i.e. it is considered that they belong to the same shoot and were separated due to some occlusion.

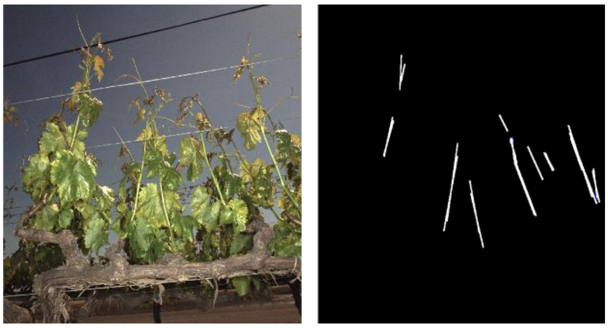

(a) (b)

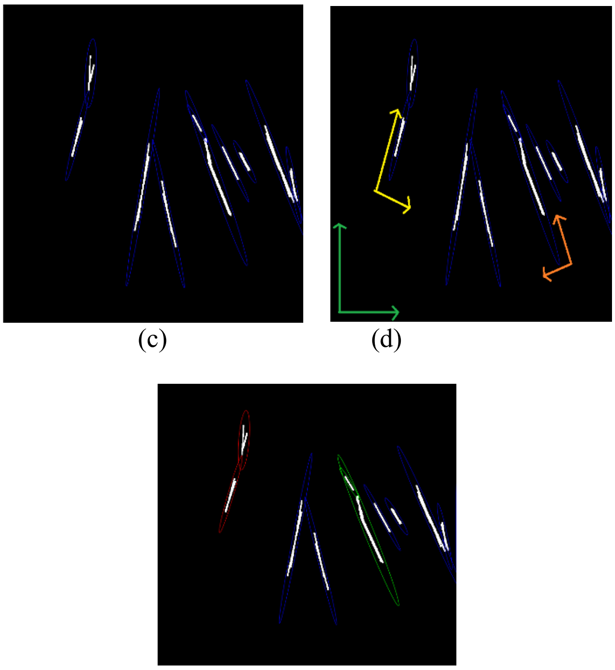

(c) (d)

(e)

FIGURE 7 (a) Initial Image (b) Binary mask from Hough Transform (c) Ellipse fitting on binary mask (d) Coordinate system transformation (e) double detections removed

4. Leaf Count Estimation

For leaf count estimation we proceed with the color and depth segmented image obtained after stage 3.2. Blob analysis is performed over the binary mask of this color and depth segmented image, to obtain blobs of various connected parts of the binary mask. Rectangles are fitted to the connected components generated from the algorithm shown in fig.8(a). Centroid of the blob is the centroid of the rectangle. Since blobs may be of various shapes and sizes, it is common that many of the rectangles might be overlapping, partially or even completely. An instance is shown in fig 8.

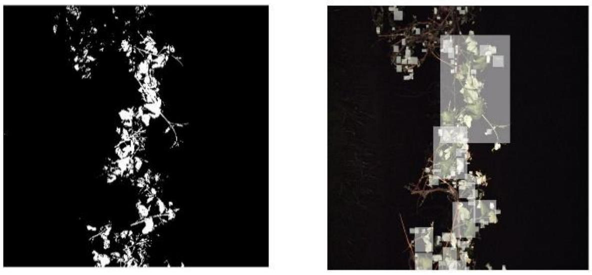

(a) (b)

FIGURE 8 (a) binary mask of the segmented image. (b) Rectangles fitted to various blobs detected in th eimage.

Now we proceed with leaf count estimation in a step by step method.

4.1 Candidates for Small Leaves

All the blobs that have an area between 500 px^2 and 1000 px^2 are considered to be candidate blobs for small leaves in a vine. The center coordinates of the fitted rectangle are dumped in a queue. Let it be Q1. These blobs are covered with a black mask which is of the size of their respective fitted rectangles. This is done so that these blobs are not taken into account in later stages. For display purposes these blobs are shown in blue color in Fig.9. Some of these blobs might not be leaves, or may be part of a relatively bigger leaf. Such instance are removed at later stages.

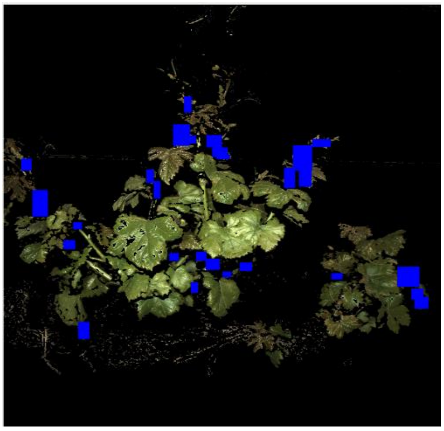

FIGURE 9. Blobs selected at first stage

4.2 Shoot Removal

Next step is to remove the shoots from the Image, so that only laeves remain. It is not possible to remove all instances of shoots completely from the image. But we can do some morphological operations to remove as many as possible. For that we create a Morphological Structuring Element of shape '*Disk*' and a size of radius 20 px. This method removes nosie speckles, but more importantly it removes the small linear parts of the image. Hence, it effectively erodes away the instances of shoots that might not be lying over a leaf, i.e. shoots whose neighboring pixels are black.

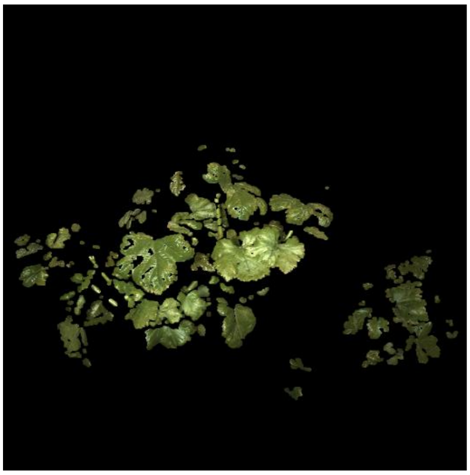

FIGURE 10. Morphologically opened image

Note that we use morphological opening and not erosion alone, because we have not selected leaf candidates of size greataer than 1000 px^2 yet. An erosion operation might erode away the small leaf candidates and shoots alike.

4.3 Candidates of leaves in meduim sized blobs

Then, next step is to make the binary mask of the image shown in Fig.9. Then blobs are again detected over this bibary mask. The blobs that have an area of 800 px^2 to 6000 px^2 are taken as individual leaves and are covered with black masks. This size range is decided emperically. The centroids of these blobs are dumped in the queue Q1. Some of thse centroids might be repetitions. But that will be addressed to at later stage. These blobs are masked with a black mask, so that they are taken into account in later stages of algorithm. The masked part of the image is shown in the figure below. It is shown in green for ease of visualization.

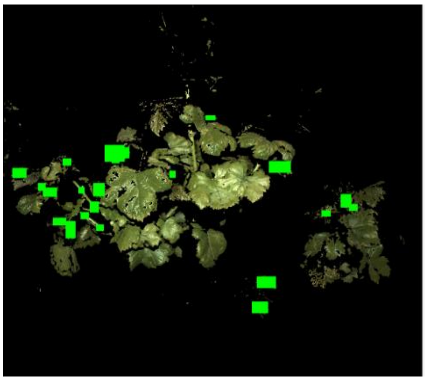

FIGURE 11. Blobs for leaf candidates at second stage

4.4 Candidates of leaves in large blobs

At this point we are left with an inamge that looks like fig.10. Next step is count the big leaves. Now the region of interests are the bounding boxes with an area greater than 6000 px^2. Each bounding box at this point is treated seperately. The coordinates of all the boubding boxes are noted down and stored in a separate queue, say Q2. The imge which we obtain at stage corresponding to Fig.18 is turned into a grayscale image. The greyscale image is passed through the morphological operation, called Erosion.

Erosion induces gaps between the bigger leaves or the cluster of leaves that a blob might be depicting. Fig.11 shows the eroded image.

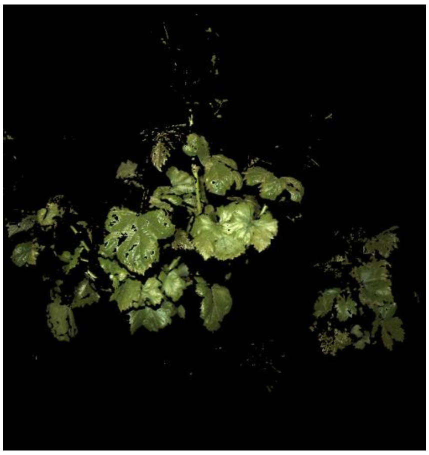

FIGURE.10 Image resulting when small and medium blobs are masked

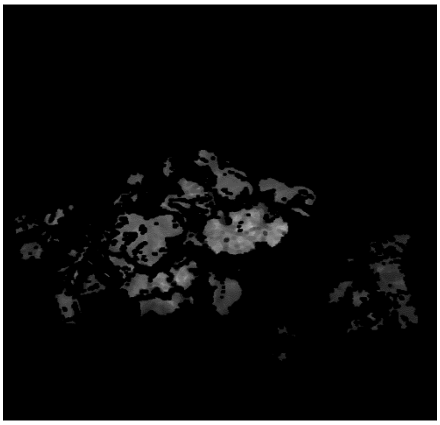

FIGURE.11 Eroded image

After erosion the bounding box coordinates are taken oout of Q2 and the eroded image is cropped at the coordinate locations, to produce several images. Some of those crops are shoen in Fig. 12

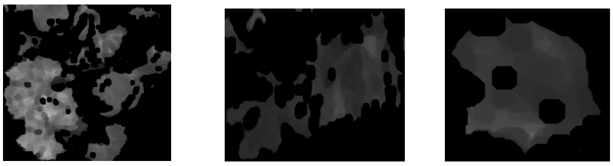

FIGURE. 12 Crops at coordinates of bounbing boxes in Q2 queue

After this, each crop is converted into a binary image and blob analysis is done over them. This technique in practice, helps us to differentiate leaves among a cluster of leaves, that the blob corresponding to rectangle in queue Q2 might be depicting. The centroids of the blobs obtained after blob analysis in each crop are dumped into the queue Q1.

At this stage the centroids in Q1 represent candidate leaves in various sized blobs in the image. Hence, by plotting the coordinates in Q1 over the original image yields an image shown in Fig.13.

This result looks disasterous due to all the multiple detections of same leaves. Hence, in the next section a way to tackle it is discussed.

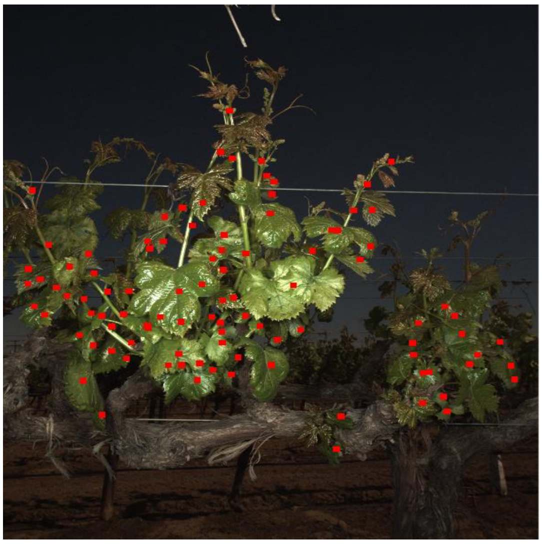

FIGURE. 13 All the candidate leaf positions plotted over the original image

4.5 Removing Multiple Detections

From previous steps, we have a queue data structure, Q1 that has the centroids of all the perspective leaf candidates. The length of this queue gives us the total number of leaf proposals. Since multiple proposals might belong to the same leaf, there are multiple-dtections and this reduces accuracy.

The following algorthm is implemented to get rid of multiple detections:

```
• Initialize 1-D arrays *Leaf* and *Repeat*
• Copy all coordinates from Q1 to 1-D array q1
• While Q1 *is not empty*
    o Dequque a coordinate pair from top of Q1
    o Make a crop of 400x400 px, in around the coordinate pair, in the binary of thresholded image.
    o White pixels represent traversable regions and black pixels represent non-traversable regions fro geodesic distance transform computation.
    o For *all remaining coordinate pairs in Q1*:
        ◆ If *any pair lies in the crop :*
            ▪ Compute geodesic distance transform between the centroid of crop and the coordinate pair.
            ▪ Skelettonize the transform.
            ▪ Calculate the pixel length along the skeletonized transform.
            ▪ Calculate the euclidean distance among the two coordinates
            ▪ If *the ratio* $\frac{Euclidean\ \ Distance}{Skeletonized\ \ Path\ \ Length} > 1.3$ :
                ❖ Copy the centroid coordinates to the array *Leaf*
            ▪ Else :
                ❖ Copy the centroid coordinates to the array *Repeat*
        ◆ End If
    o End For
• End While
```

The following steps explain the algorithm in detail:

1. Extract the coordinates from th enqueue, ony by one from the top.
2. Crop a 400px X 400px region from the binary mask of the image. The white pixels in the mask correspond to the traversable region and black correspond to the non-traversable region.
3. In the crop, we look if any other coordinate from the queue lies in it too.
4. If yes, then we conpute the geodesic distance transform between the two points. This gives us the maximum possible paths with minimum distance between the two points.
5. If no, then we pass to the next point in the queue and repeat the step 3.
6. If, point is present, then we skeletonize the geodesic distance. The number of pixels in it gives the minimum path length along the mask.
7. If the ratio of euclidean distance to the path length is more than 1.3, that means path length is curvy and there is no straight line path among the two points. This means the point sbelong to different leves.
8. If the ratio is below 1.3, it means that the points more or less lie on the same leaf. Then one of them is set to (0,0)
9. Steps 2 t 8 are repeated for all the points.

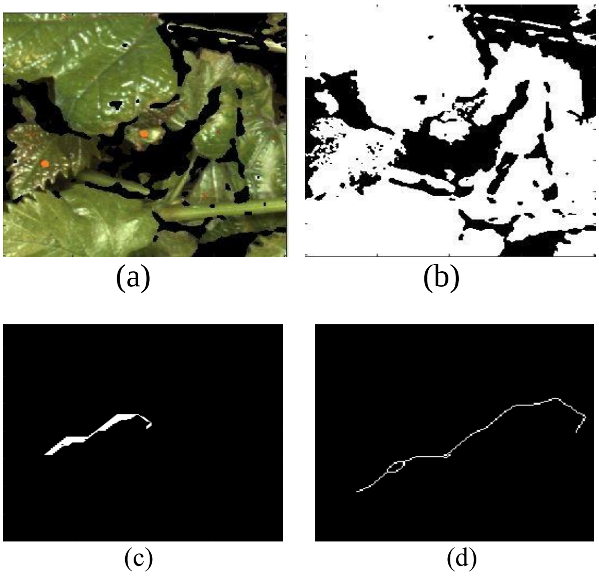

FIGURE. 14. (a) Two points of interest, (b) The binary mask of the crop, (c) Geodesic distance transform along the binary mask among the two points and (d) The Skeletonized path(zoomed for clarity)

Fig.14 Shows an example where the two candidate points belong to deifferent leaves. In this case the pixel length of skeletonized path is greater than the euclidean distance among these points. This suggests that the path between the two points is wavy, due to breaks between the binary mask, between the two points. These breaks are due to discontinuities between the leaves. So, the two points belong to different leaves. Hence, none of the candidates are eliminated.

Whereas, Fig. 15 depicts an example where both the candidates belong to the same leaf. The pixel length of the skeletonized path is not substantially greater than the euclidean distnce aming the two points, it may even be exactly the same in case of staright lines. In other words the ratio $\frac{Euclidean\ Distance}{Skeletonized\ Path\ Length} < 1.3$ (the constant 1.3 is emperically decided). This shows that an almost straight line path exists between the two points, along the binary mask. This suggests that both the point belong to the same leaf. Hence the point that is not the centroid is eliminated.

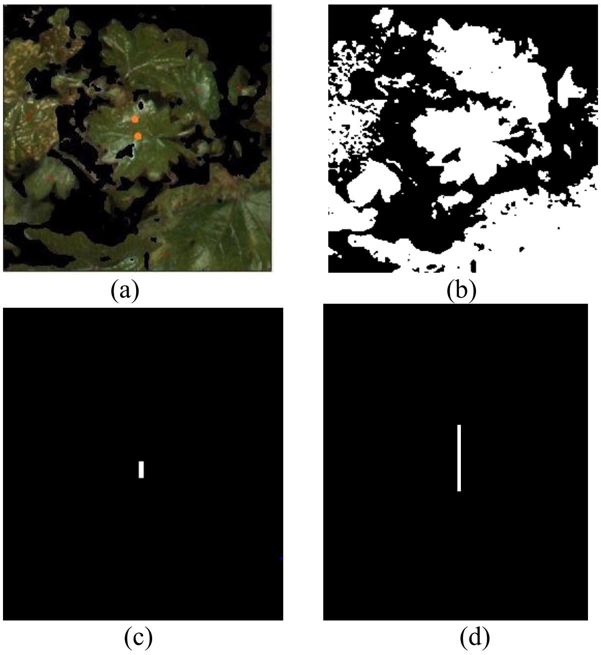

FIGURE. 15. (a) Two points od interest, (b) The binary mask of the crop, (c) Geodesic distance transform along the binary mask among the two points and (d) The Skeletonized path(zoomed for clarity)

Fig.16 shows the fimal result for leaf count. The points that didn't get eliminated are shown in yellow and the eliminated points are shown in red color. Hence, the number of yellow points is the final leaf count. The algorithm gives a leaf count of 59 as compared to 105 prior to removal of double detections. The ground truth for the image, which is 52, is manually labelled. Hence, the accuracy increases manifold.

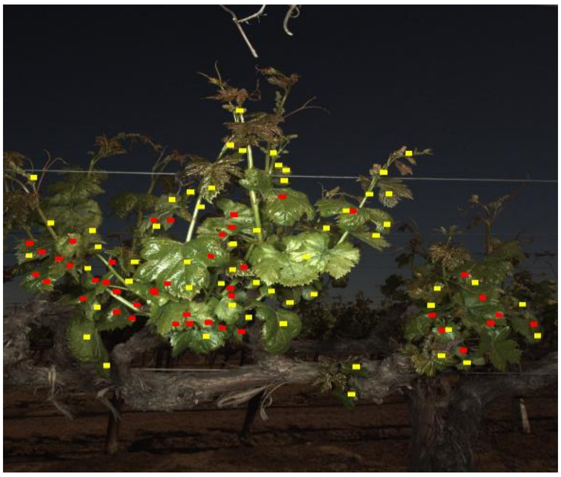

FIGURE. 16. Eliminated double counts

5. Leaf Area Estimation

The image obtained after background and color segmentation is used as the starting point for leaf area estimation. From the disparity map, shown in Fig.1 is used to calculate the depth of each and every pixel in rectified image. From emperical study, we can safely conclude that, a square object of area 100 cm^2 at a calibrated distance of 50 cm from the camera, when projected over the focal plane of the camera, covers the image plane such that each pixel depicts an area of 0.0005351158 cm^2 in real world coordinates.

This Area Per Pixel(App) increases as a square function of distance from the camera. Hence if the distance of the object from the camera is x cm, then the area represented by each pixel at that distance will be $\frac{x}{50} * 0.0005351158^2$. Hence, the real world area is given by the following

$$Area = \sum_{i=1}^{N} \left(A_{PP} * \ \left(\frac{D_i}{50}\right)^2 \right) \qquad (6)$$

Where,

- N = number of green pixels
- D_i = Depth of each pixel
- A_{pp} = Area per pixel at depth of 50 cm

The following flow-chart explains the process:

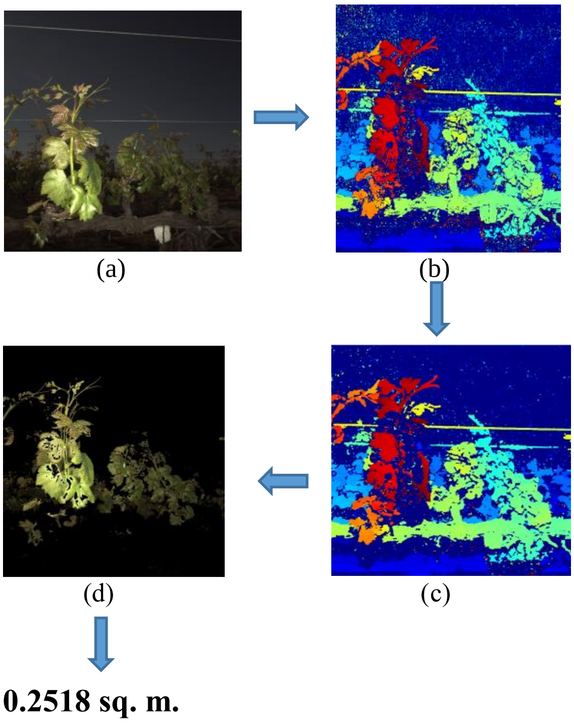

FIGURE. 17. Leaf Area Estimation flow-chart (a) Rectified image, (b) Disparity Map, (c) Median filter application for smoothening and (d) Image for area calculation

6. Results and discussion

Our imaging system consisting of a pair of RGB stereo cameras and a pair of flashes is setup to optimize low motion blur, capture increased depth-of-focus, and uses low illumination power for fast-recycle times permitting high-frame rates. This camera and illumination design maintains high image quality at high vehicle velocities and enables deployment on large scales. The imaging system is mounted onto the side of the farm vehicle facing the fruit wall. Depending on the size of the fruit zone a distance of 0.9 to 1.5m is maintained between the imaging system and the fruit zone. The farm vehicle was driven at 1.5m/s through each row and the images were captured at 5Hz.

The datasets were collected from different vineyards across California. In each field calibration tags were put up randomly in 10 rows and for 2 vines in each of the selected rows. For shoot count estimation the ground truth was measured on these rows manually by 2 people. Whereas, for leaf area measurement the sensor data collected from a PAR sensor was used as ground truth. The sensor values were regularly sampled from start to end of a tag. Canopy light penetration as well as ambient light data were recorded. These values were used to find the correlation between the value $1 - \frac{Canopy\ light\ penetration}{Ambient\ light}$ and algorithm output.

For testing the accuracy of leaf count estimation algorithm, 32 images from a dataset containing the images of Flame Seedless vines were randomly selected. These images were hand labelled for marking and counting visible leaves in the images.

Fig.19 and Fig.20 show the linear regression curves for leaf count estimation and leaf area estimation respectively. The correlation coefficient for leaf count estimation is 0.798 and that for leaf area estimation is 0.69. The performance of the system for shoot count estimation can be analyzed by the F1 score given in table 1. 25 images were randomly picked and the visual shoot count in the images was done manually to obtain the F1 score.

Precision	Recall	F1 Score
0.86	0.84	0.85

Table 1. Precision recall and F1 score

Each vine has an average length of 14 feet. Which then converts to 4.2672 meters. Thus this helps to get ground truth shoot count per meter for each of the vine. Then visual counts for these images covering calibration vines was divided by difference of real world x coordinate values obtained from the disparity map at both the ends of calibration plots to get visual shoot count per meter.

To find the correlation between visual shoot count per meter and ground truth shoot count per meter, we use Pearson's correlation. Correlation value was calculated to be 0.88. The correlation graph is described in figure 18.

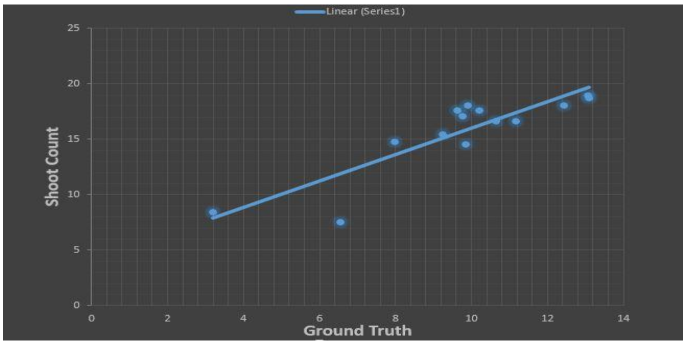

FIGURE 18 Correlation graph for ground truth shoot count per meter vs algorithmically calculated shoot count per meter

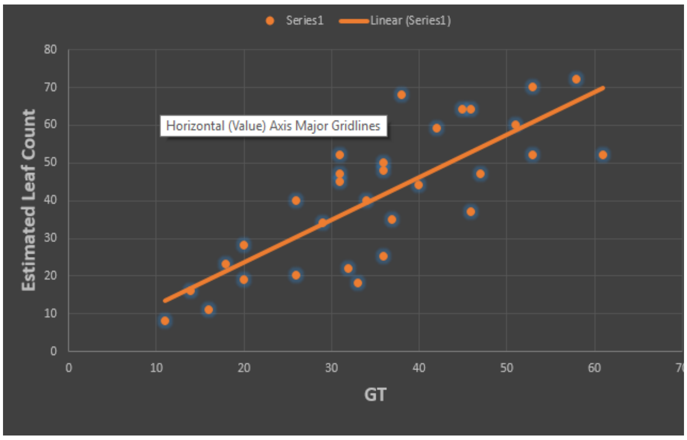

FIGURE. 19 Linear Regression Curve for Leaf Count Estimation

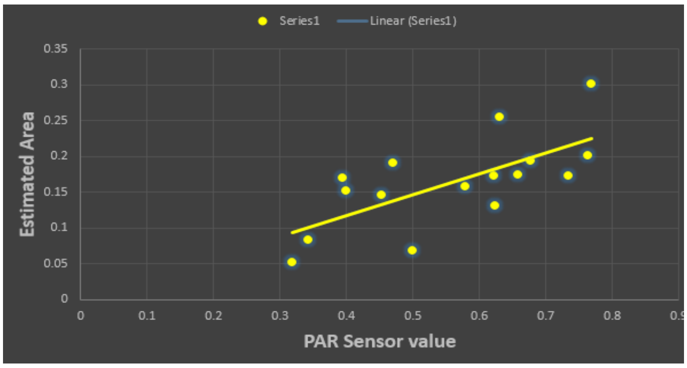

FIGURE. 20 Linear Regression Curve for Leaf Area Estimation

7. Conclusion

It has been known that shoot density plays an important role in grower decision making process regarding storage, shipment, crop management and market price. Thus if there exists an algorithm that can accurately estimate this parameter, it can add economic value to the vineyard industry.

The quantitative analysis shows that there exists a correlation between the visual shoot count per meter and the actual shoot count per meter. The algorithm is validated by a high F1 score of 0.85 and the existence of correlation between visual count and ground truth can be validated by the correlation coefficient value of 0.88. And for leaf area analysis, it can be deduced that, there exists a correlation between the PAR sensor data and estimated leaf area. The low value of the R1 correlation coefficient might be attributed to the variance in PAR data collection and vine image collection. Further study is required to resolve this discrepancy. The work also shows that the leaf count estimation algorithm has a correlation coefficient of 0.798, with the manually *ground truthed* images. The future work would estimate the correlation between the total number of leaves counted in a vine and the algorithm output.

8. Acknowledgement

This work is supported in part by the US Department of Agriculture under grant number 2015-51181-24393 and the National Grape and Wine Initiative info@ngwi.org. The authors would like to thank the following people who assisted in collecting the data for this paper; Maha Afifi, Franka Gabler and Kaan Kurtural and his lab at UC Davis.

References

[1] Z. Pothen and S. Nuske. “Texture-based fruit detection via images using the smooth patterns on the fruit”. In Proceedings of the IEEE International Conference on Robotics and Automation, May 2016.

[2] Stephen Nuske, Kyle Wilshusen, Supreeth Achar, Luke Yoder, Srinivasa Narasimhan, and Sanjiv Singh. “Automated visual yield estimation in vineyards”. Journal of Field Robotics, 31(5):837-- 860, September 2014.

[3] K.Ma College of Biosystems Engineering and Food Science, Zhejiang University, “A Survey of Stem Detection Algorithms and A New Algorithm Based on Monte Carlo Method” Neural networks 6.6 (1993): 801-806.

[4] Hung, Chia-Che, et al. "Orchard fruit segmentation using multi-spectral feature learning." Intelligent Robots and Systems (IROS), 2013 IEEE/RSJ International Conference on. IEEE, 2013.

[5] Ruiz L A, Molto E, Juste F, et al. Location and characterization of the stem-calyx area on oranges by computer vision [J]. Journal of agricultural engineering research, 1996, 64(3): 165-172.

[6] Paproki, Anthony, et al. "Automated 3D segmentation and analysis of cotton plants." Digital Image Computing Techniques and Applications (DICTA), 2011 International Conference on. IEEE, 2011.

[7] Alejandro F. Frangi, Wiro J. Niessen, Koen L. Vincken and Max A. Viergever. Multiscale vessel enhancement

filtering. Lecture Notes in computer Science, 1496: 130—137, October 1998.

[8] Richard O. Duda and Peter E. Hart. Use of the Hough Transformation to detect lines and curves in pictures. Communications of the ACM, 15:11—15, January 1972.

[9] Dunn, G., & Martin, S. (2004). Yield prediction from digital image analysis: A technique with potential for vineyard assessments prior to harvest. Australian Journal of Grape and Wine Research, 10: pp 196198.

[10] Rabatel, G, and C Guizard. (2007). Grape berry calibration by computer vision using elliptical model fitting. European Conference on Precision Agriculture, 6: pp. 581- 587.

[11] Alenyà, G., et al. "Leaf segmentation from ToF data for robotized plant probing." *IEEE Robotics &Automation Magazine* (2012).

[12] Xia, Chunlei, et al. "In situ 3d segmentation of individual plant leaves using a rgb-d camera for agricultural automation." *Sensors* 15.8 (2015): 20463-20479.

[13] Li, Chunming, Jundong Liu, and Martin D. Fox. "Segmentation of edge preserving gradient vector flow: an approach toward automatically initializing and splitting of snakes." *2005 IEEE Computer Society Conference on Computer Vision and Pattern Recognition (CVPR'05)*. Vol. 1. IEEE, 2005.

[14] Giuffrida, Mario Valerio, Massimo Minervini, and Sotirios A. Tsaftaris. "Learning to count leaves in rosette plants." (2016): 1-1.

[15] A. Coates, A. Arbor, and A. Y. Ng. An analysis of single-layer networks in unsupervised feature learning. International Conference on Artificial Intelligence and Statistics, pages 215–223, 2011.

[16] C. Elkan. Using the triangle inequality to accelerate k-means. In International Conference on Machine Learning, pages 147–153, 2003.

[17] Xia, C., Lee, J. M., Li, Y., Song, Y. H., Chung, B. K., & Chon, T. S. (2013). Plant leaf detection using modified active shape models. *Biosystems engineering*, *116*(1), 23-35.

[18] Diago MP, Correa C, Millán B, Barreiro P, Valero C, Tardaguila J. Grapevine yield and leaf area estimation using supervised classification methodology on RGB images taken under field conditions. Sensors. 2012 Dec 12;12(12):16988-7006.

[19] Knyazikhin, Y.; Martonchik, J.V.; Diner, D.J.; Myneni, R.B.; Verstraete, M.; Pinty, B.; Gobron, N. Estimation of vegetation canopy leaf area index and fraction of absorbed photosynthetically active radiation from atmosphere-corrected MISR data. *J. Geophys. Res. Atmos.* **1998**, *103*, 32239-32256.

[20] Haboudane D, Miller JR, Tremblay N, Pattey E,Vigneault P. Estimation of Leaf Area Index using Ground spectral measurements over Agriculture crops: Prediction capability assessment of optical indices. Can. J. Remote Sens. 2004;23:143-62.

[21] Mohammed Amean, Z., et al. "Automatic plant branch segmentation and classification using vesselness measure." Proceedings of the Australasian Conference on Robotics and Automation (ACRA 2013). Australasian Robotics and Automation Association, 2013.

[22] Fit an Ellipse to a Region of Interest (September 22, 2016). Retrieved from : http://www.idlcoyote.com/ip_tips/fit_ellipse.html